

Miniaturized novel quintuple-band microstrip patch antenna for K-band application

Kumari Mamta^{1*} and Raj Kumar Singh²

Associate Professor, Department of Physics, Nalanda College of Engineering, Chandi, Nalanda-830108, India¹

Assistant Professor, University Department of Physics, Ranchi University, Ranchi-834008, India²

Received: 12-August-2023; Revised: 14-April-2024; Accepted: 17-April-2024

©2024 Kumari Mamta and Raj Kumar Singh. This is an open access article distributed under the Creative Commons Attribution (CC BY) License, which permits unrestricted use, distribution, and reproduction in any medium, provided the original work is properly cited.

Abstract

Microstrip K-band antennas are popular because they are inexpensive, easy to integrate, and lightweight. This paper aimed to present a novel quintuple-band scaled down microstrip patch antenna (MPA) with a substrate measuring 28 mm by 25 mm, designed using 1.6 mm thick fire retardant 4 (FR4) dielectric material for K-band application. All simulation work was performed with Ansoft high frequency structure simulator (HFSS) antenna simulation tool, and the results were confirmed using experimental data from the constructed prototype. It features two identical L-shaped patches and two U-shaped patches with different sizes. The antenna was fed via the microstrip line feeding technique. Two U-shaped patches were separated by U-shaped slits, allowing the antenna to work in quintuple-band applications. The antenna patch dimension was calculated using normal microstrip formulae, and the size was then optimised. Quintuple resonant frequencies occurred at 21 GHz, 24 GHz, 28 GHz, 31 GHz, and 34 GHz. The average return loss, scattering parameter (S11) was found to be less than -10 decibel (dB), and the average voltage standing wave ratio (VSWR) value was 1.548 for the quintuple band. The gain was 6.13 dB, and the bandwidth was 0.5 GHz, which is adequate to link to neighbouring radiators with varying heights of catch angle 35°. Directivity created by several resonant frequencies allowed the antenna to radiate equally well in all directions. The modelling and observed findings agreed almost perfectly. The results achieved are comparable to mobile communication, satellite communication, military applications, defence monitoring radar, and other fifth and sixth generation (5G/6G) communication requirements in the K band. Future research may focus on increasing bandwidth and achieving various resonance frequencies in additional operating bands for microstrip patch antennas.

Keywords

Microstrip patch antenna, Multiband, Slot, Substrate, Loss tangent, Antenna radiation pattern.

1. Introduction

1.1 Background

The introduction of wireless communication devices has sparked interest in small-size antennas. Additionally, the demand for multiband frequency operating antennas with various patterns is felt to fulfil the requirements and problems of fifth- and sixth-generation (5G and 6G) communications. Aside from excellent radiation efficiency and anti-interference performance, factors such as a greater frequency band, lower size, and ease of installation are also required. Therefore, multiband functioning and antenna miniaturization are necessary [1–3].

Present work is important in terms of its quest for multiband features, good gain and bandwidth, stable radiation pattern and directivity, size miniaturization, and an application for K-band communication. Microstrip patch antenna (MPA) is an obvious option because of its ease of integration, maintenance, and several other distinguishing and appealing properties. MPA consists of three layers. The top layer is often a metal foil, known as a radiating patch. Ground is the lower part, whereas dielectric is the middle part. Radiation of electromagnetic wave of the MPA is due to in-phase addition of bordering E-fields on its perimeter. Microstrip antennas are more small, low profile, inexpensive, and lightweight than typical microwave antennas, allowing them to satisfy miniaturization criteria. The patch antenna's qualities may be optimized by a variety of adjustments. Future wireless technologies, including 6G, are now being

*Author for correspondence

researched in addition to 5G. As data rates and applications progress, sophisticated millimeter wave antenna designs will be required [4–7]. The dielectric loss can be easily reduced by utilizing a substrate with a low loss tangent. Radiation loss is decreased by employing a thin dielectric sheet, as bulkier substrates have a greater surface current.

Millimeter wave patch antennas exhibit reduced penetration loss and free space propagation loss. Microstrip antennas, on the other hand, must be considered multiband antennas due to their inherent bandwidth limits. The MPA design employs band notch characteristics to provide proper band separation and antenna performance without interference [8, 9]. Radiating patches and ground planes are filled with parasitic gaps and slits to reduce antenna size.

1.2 Challenges

The researchers' challenge is to build a multi-band frequency operational microstrip antenna for (5G/6G) wireless communication applications like the internet of things (IoT), artificial intelligence (AI), blockchain technology, and cellular communication. These issues are exacerbated when one measure worsens while the other improves. As a result, efforts must be made to ensure that the antenna characteristics have the best possible reach and value. Researchers face challenges in achieving lower free space propagation loss, dielectric loss, conductor loss, and radiation loss while maintaining antenna features and properties like radiation efficiency, directivity, return loss coefficient, gain, bandwidth, impedance, voltage standing wave ratio (VSWR), and so on.

1.3 Motivation

Many researchers worked hard to develop a multiband operating suitable antenna. Integrating many bands into one antenna is critical in a variety of applications. An antenna with many bands is required for cognitive radio services. MPA demonstrates a variety of capabilities and multiband operational capability. The relative permittivity of the substrate affects size of patch antenna, frequency response consistency and level of stability [10]. Because MPAs are simple to utilise with integrated circuits, they are considered as the ideal antenna design. A good gain, larger bandwidth, adequate reflection coefficient, increased efficiency are all features of such an antenna to provide a viable option for the high-quality services in 5G spectrum [11–13]. Millimetre waves have been investigated and proven to be viable for usage in 5G and next-generation

communication systems, including current AI-based gadgets. Millimetre wave applications exist in numerous bands, the K-band receiving a lot of research interest [14–19]. The majority of research is focused on improving the antenna's impedance bandwidth, steady radiation pattern, directivity, stabilised gain, and cost-effectiveness. The proposed antenna is quintuple-band, operating at frequencies of 21 GHz, 24 GHz, 28 GHz, 31 GHz, and 34 GHz. All resonance frequencies, with the exception of the centre one at 28 GHz, are around 3 GHz apart, which is sufficient for 5G/6G connectivity. The design techniques and performance characteristics are provided. The low-profile antenna is made from a fire retardant 4 (FR4) Epoxy substrate having loss tangent of 0.025 and relative permittivity $\epsilon_r = 4.4$. FR4 is utilised as a substrate due to its electrical properties, moisture resistance, superior electrical insulation, high strength-to-weight ratio, accessibility, and low cost. The substrate height is adjusted to the typical 1.6 mm. By photolithography method, the proposed antenna can be easily prepared.

1.4 Objectives

Main objectives of the proposed work are-

- (a) To design, simulate and develop a multi frequency operational MPA suitable for K-band applications.
- (b) To validate the working results of the antenna with the results obtained from simulation and optimization.

1.5 Contributions

In this research, attempt is made to address the demand for multifrequency operation microstrip antennas in the current and future generations of wireless communication. After achieving size and feature optimisation with high frequency structure simulator (HFSS), antenna prototype was created with the highest accuracy possible within the available technological framework and assessed its characteristics using a vector network analyser (VNA). The results as measured in the laboratory compares very largely with the simulated values, pointing towards the fact that it is suitable for K-band applications.

Paper structure is like this. The section following this is on the review of works done in this field. Section 3 discusses approach used for the determination of dimensions of the antenna elements utilizing a variety of fundamental and conventional formulae. The simulated and measured findings are described in section 4. Section 5 reports results and limitations of the presented work. The next section following this

discusses the conclusion along with scope for further work. This section also includes a relative study of recommended antenna with a few published works in this field.

2. Review of literature

In MPA, U-slot is primarily taken for enhancing bandwidth. Triple bands are achieved respectively with 1.6 mm and 0.6 mm thick dielectric material and the bandwidths reported are less than 1 GHz [20]. Many designs and analytical strategies for enhancing performance have been covered in research papers. Use of metamaterial provides bandwidth ranging from 1 to 4.2 GHz, gain of 1.5 decibel relative to isotropic (dBi). The efficiency being 35% at the operational frequency, using substrate Rogers RO4003. The use of second planar slot improves gain and efficiency respectively by 2 dB and 25%. [21]. Non-symmetric patch has realized axial ratio of 3 dB in a three band antenna by using etching slots and stubs along two axes [22]. Double square radiating patch designed to rule out the interference from wireless fidelity (WiFi) bands and Bluetooth, fed through a transmission line has achieved a notched features at global positioning system (GPS), Bluetooth and WiFi frequency bands. The radiator is enveloped by a ground-plane conductor with an H-plane dielectric slit embedding at 90° rotation. This has led to an impedance bandwidth of 2.55 GHz at VSWR less than two. Radiation pattern of antenna being omnidirectional [23].

MPAs are widely distributed and have distinct characteristics employing various alphabetical slots like E, H, U-slots. A carved planar antenna with an E-shaped unit cell, designed specifically for wide band and microwave systems, claims 5.3 dBi gain and an efficiency of 85% at 1 GHz [24]. Even a slot patch antenna targeted for 5G application using printing fabrication has achieved a gain of 5 dBi at three frequency bands ranging from 5 GHz to 8 GHz [25]. With an area of 40 by 30 mm², a printed MPA consisting of U-slot using the second and third mode excitation is found to resonate with frequency 2 to 8 GHz [26]. MPA designed with U-slot subject to the matrix formulation calculation in the computer simulation technology (CST) environment leads to measured resonating frequency with an error less than 2% and less than 10% error in the bandwidth. The antenna fabrication is on printed board computerized numerical control (CNC) machine and the laboratory measurement is carried out using network analyser [27]. Khunead et al. [28] investigated the operation of antennas with equal-

sized rectangular patches, as well as those with and without L-shaped strips. The K band is helpful for systems that communicate over short distances. The Ka-band and Ku-band are two further divisions above and below the K-band. The Ku band is allocated for satellite communications. The Ku band frequency range is largely utilised by very small aperture terminals (VSATs), which are tiny earth stations that receive and send video and data signals via satellite networks. On the ground surface, Ku band frequencies, however, have a lesser coverage area, but can give a broader beam coverage. This band's activity reduces in damp conditions due to water droplets absorbing. Wavelengths in the Ka-band vary from 11 mm to 7.5 mm and is mainly used by high throughput satellite (HTS) services. In a shorted high order wideband mm wave antenna, with size enlargement achieved by exploiting its high order mode for easy fabrication, higher tolerance and lower cost, 18% impedance bandwidth and broadside radiation is reported. A slot is provisioned to widen the bandwidth [29]. An antenna designed, simulated, and optimised using HFSS with substrate RT5880 with relative permittivity 2.2 and thickness 0.508 mm, achieves 8 dB gain, a maximum reflection coefficient of -45 dB, spread across frequency range 27.28 GHz to 28.71 GHz. CST is utilised to validate HFSS simulation results [30]. An effort beyond Ka band at resonant frequency 47.2 GHz with an inset feed line and a modified ground plane resulted in a broad bandwidth of around 2.8 GHz and a return loss of -24.71 dB [31]. A compact ultrawide antenna with dual band is obtained using FR4 substrate for wide band applications [32]. Use of different substrate material finds optimum radiation efficiency for FR4 material at 29 GHz for 5G communication. Use of Rogers RT/Duroid 5880 and Taconic thin layer chromatography (TLC) independently makes antenna around 90% efficient. FR4 obtains high bandwidth of 2 GHz, whereas Rogers RT/Duroid material delivers a reflection coefficient of -36 dB, gain of 5.9 dB, VSWR of 1 and a bandwidth of 1.8 GHz [33]. Reduction of mutual coupling extends the bandwidth marginally with an improvement in gain for K-band applications. The antenna is a modified compact antipodal broadband Vivaldi antenna array with eight antenna components connected by a 1-to-8 power divider. Multiple notch structures are placed into the ground plane to mitigate the effects of reciprocal coupling. Isolation between antenna elements can produce a gain boost of about 37.3 dB while also improving impedance bandwidth. Arrays support sixteen elements in the magnetic field plane design. This reduces influence of mutual coupling while

improving bandwidth and return loss. Amplitude distribution is homogeneous with maximum gain of 19.88 dBi [34, 35]. Microstrip parasitic patch antenna with metalized elliptical stripline that has achieved around six percent fractional bandwidth in the K-band frequency range employing 6-way power divider. Measurement results report gain of 21.4 dBi [36]. Two U-shaped slot patch antenna with 2x2 array results 13 dBi gain for a wideband communication system. The antenna structure is simplest in its form and comprises of a patch, two U-shaped slot and the ground plane. When the antenna is arrayed to 2x2 the gain realized reach to 13 dBi [37]. Resonant frequency of 28 GHz is studied using Huygens source microstrip antenna with a radiation efficiency of 81% using planar multilayered source. The antenna is broadside radiating and constructed with multilayer printed circuit board (PCB) technology. The device is integrated using an electric Egyptian axe dipole via a coaxial dipole radiator. Linearly polarised (LP) and circularly polarized (CP) versions are tested. The LP system offers peak realised gains of 3.77 dBi and front-to-back ratios (FTBR) ranging from 7.16 to 33.92 dB, whereas the CP system has peak realised gains of 2.03 dBi and an FTBR of 26.72 dB. The two systems had radiation efficiencies of 81.14% and 73.4%, respectively. The fractional impedance bandwidth is -10 dB in both systems, and the specific absorption rate is determined to be quite low [38]. A high gain performing antenna designed for K band application has 21 dBi gain and bandwidth of 1 GHz. The antenna is configured with 6x5 near coupled planar array [39]. Another Ka band compatible antennas has side lobe gain of 21 dBi and 6.5 dBi in the K-band frequencies. The antenna utilises planar microstrip technology and is constructed with one-fifth of a millimeter thick Rogers-5880. The antenna array consisted of a microstrip patch with two-pronged fork configuration. The realised gain for a single radiator is 7.6 dBi. CST Microwave Studio was used to model and optimise antenna array designs of sizes 8×8 , 8×16 , and 8×32 . The proposed multiple-input-multiple-output (MIMO) configuration has four radiating components, each having Hewlett-Packard (HP)-shaped architecture. The antenna has a measured wide bandwidth of 36.83-40.0 GHz and a peak gain of 6.5 dB. The electromagnetic radiator emits well at the desired frequency range [40, 41]. A study exploring the effect of variation of height of conducting patch on the performance of MPA reports 9.47 dBi gain and a performance efficiency of 90.1%. This mathematical model depicts an MPA with air as substrate material enclosed in a volumetric size of

$5.43 \times 4.54 \times 0.5 \text{ mm}^3$ with resonance at K-band frequency. The effects of various conducting materials and thicknesses of middle layer of dielectric material on various antenna parameters are reported. Designed antenna achieved bandwidth of 1.72 GHz [42]. A compact high bandwidth ultrawide band MPA has reportedly achieved around 103 GHz bandwidth, using a 50-ohm tapered microstrip line, allowing catchment of different wireless applications such as worldwide interoperability for microwave access (WiMAX) and wireless local area network (WLAN) [43]. Dual band patch single-element antenna designed to resonate at 38 GHz and 60 GHz has minimum return loss values at -42 dB and -47 dB. This is accomplished via electromagnetically connected patches. The antenna's omnidirectional radiation patterns and balloon-like form for both bands qualify it as a potential choice for a MIMO system composed of a number of orderly assigned components [44]. A K-band millimetre wave tri-band antenna designed to perform at 26 GHz, 32 GHz and 39 GHz resonant frequency, suitable for corridor indoor line of sight condition, has realized well shadow fading behaviour. In the two antennas configuration a horn antenna is used in the transmission and a horn and omnidirectional antenna used in the reception [45]. A quad-band millimetre wave MPA employing RT Duroid 5880 substrate, employing tapered line feed and operating at resonant frequencies in K- and beyond K-band has achieved a reflection coefficient of -19.5 dB [46]. Planar MIMO radiator explored for 5G communication with use of different substrate has realized wide bandwidth with high gain and narrow directional radiation. Planar MIMO topologies studied include slot, defective ground structure, coplanar waveguide (CPW), tapered/Vivaldi, meta surface/metamaterial, dielectric resonator, transparent, and flexible/wearable antennas. The impact of slots, decoupling structures, and partial ground on bandwidth, isolation level, and impedance matching is reported [47]. A quad-band multi-polarized monopole antenna made up of a combination of T- and L-shaped stubs was studied with parasitic multistubs in Y-direction behind patch antenna. This reached resonance at four frequencies less than 10 GHz. Measured impedance bandwidths are in MHz making it suitable for Bluetooth, WLAN and X-band satellite applications. Quadband features are obtained. At the first, second, and third resonance bands, the electric field radiation is along Y-direction, whereas at the fourth resonance band, it is slanted $+45^\circ$ [48]. Fertas et al. [49] described a miniaturized five band antenna, capable of functioning at five resonant frequencies. The antenna

design includes and exploits the features of using L-slots and 50 CPW. Pentaband operation is realized in sub-10 GHz frequency range, maintaining a size of 27.4×24 mm². Another work on K band mm wave antenna with designed dimension of 4.46 mm × 6.6 mm with RT Duroid substrate having resonant frequencies spread over 27 GHz to 57 GHz, has gain varying from 7.7 dBi to 10.2 dBi [50]. A three-band resonant frequency (28 GHz, 40 GHz and 47 GHz), antenna using FR4 epoxy dielectric material has gain of 5.64 dBi to 8.7 dBi [51].

Most researches have concentrated on dual, triple, and quad band resonant frequencies. There have been very few studies on the quintuple band (five bands). Therefore, the current study is relevant to finding improvised solutions for the needs of multi frequency operation, particularly five bands, of antennas for millimeter wave 5G and next generation wireless communication.

3.Methods

3.1Antenna design and configuration

An MPA is a metal patch put at ground level with a dielectric material in between. These antennas are tiny and produce very little radiation. Photo-etching is used to connect the radiating patch and feeding lines to the dielectric substance. In the photo-etching technique, also known as chemical etching, chemicals and photoresists were used to remove a specific section of the metal according to our design. The etching process consisted of planning, preparing the material and photoresist coating, developing the exposed item under UV light, chemical etching, and ultimately removing the photoresists. The antenna consisted of a homogeneous 50-ohm coaxial probe. Co-axial feed is a contact technique of radio frequency (RF) power feed for antennas. Co-axial feed has the advantage of avoiding spurious radiation and attaining high bandwidth. Basic antenna Equations (1 to 7) were used to calculate the size of a rectangular patch antenna using the transmission line model. Fine tuning was accomplished by conducting experiments on conventional antenna equations and analysing the response pattern.

$$\text{width of patch}(w) = \frac{c}{2f_0\sqrt{\frac{\epsilon_r+1}{2}}} \tag{1}$$

$$L = \frac{c}{2f_0\sqrt{\epsilon_{eff}}} - 0.824h \left(\frac{(\epsilon_{eff}+0.3)(0.264+\frac{w}{h})}{(\epsilon_{eff}-0.258)(0.8+\frac{w}{h})} \right) \tag{2}$$

$$f_0 = \frac{c}{2L_e\sqrt{\epsilon_r}} \tag{3}$$

$$\text{effective length}(L_e) = \frac{c}{2f_0\sqrt{\epsilon_{eff}}} \tag{4}$$

$$\epsilon_{eff} = \frac{\epsilon_r+1}{2} + \frac{\epsilon_r-1}{2} \left[\frac{1}{\sqrt{1+12(\frac{h}{w})}} \right] \tag{5}$$

where, $c = \text{velocity of light}$, $f_0 = \text{resonant frequency}$, $\epsilon_r = \text{substrate dielectric constant}$, $h = \text{substrate height}$, $L_e = \text{effective length}$, $\epsilon_{eff} = \text{Effective constant}$, $L = \text{Length of Patch}$

If the size of ground plane is larger than the patch's dimensions by about six times the substrate thickness all around, then the ground plane follows the measurements as in Equations 6 and 7:

$$Lg = 6h + L \tag{6}$$

$$Wg = 6h + W \tag{7}$$

The proposed antenna's geometric configuration is depicted in *Figure 1*. The two U-shaped patches enabled functioning in the top two frequency bands. The planar patch was simple, consisted of two L-shaped resonators which enabled the creation of both horizontal and vertical polarised signals. Furthermore, because the rectangular patch is the best match, it is easier to alter the resonator's length. The choice of U-shaped resonator was based on the fact that adjusting the distance between the arms of a U-shape allows for a more varied distribution of resonant frequencies than quarter- or half-wavelength resonators. The middle parasitic patch enabled 28 GHz operation. Ground plane dimensions were calculated to be 28 mm × 25 mm. The selected dielectric material was FR4, 1.6 mm thick and dielectric constant $\epsilon_r = 4.4$. Planar dimension of the planned antenna was 28 mm × 25 mm. Feeding of antenna was done by a standard 50-ohm coaxial probe.

Antenna patch dimensions are mentioned in *Table 1*. This includes patch and slots geometrical dimensions and U-arm lengths. All dimensions are in millimeter (mm). Ansoft HFSS was used to assess the recommended design features, and the results were compared to and confirmed by measurements conducted on a manufactured antenna prototype. High-frequency structure simulation software, HFSS, is used to design, optimize and simulate gigahertz and terahertz frequency electronic devices.

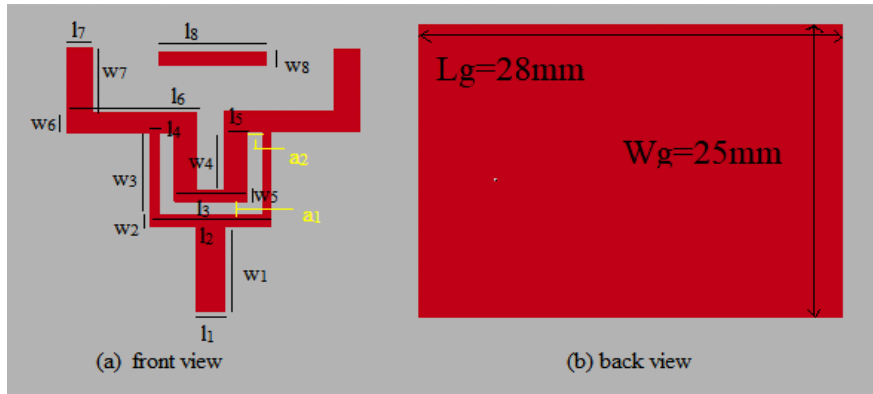


Figure 1 Geometric configuration and dimension of proposed antenna

Table 1 Antenna patch dimensions

Parameters	Dimension (mm)	Parameters	Dimension (mm)
L_g	28	w_g	25
a_1	1	a_2	1
l_1	2	w_1	6
l_2	8	w_2	0.5
l_3	5	w_3	6
l_4	0.5	w_4	4
l_5	1.5	w_5	1
l_6	9	w_6	1.5
l_7	1.5	w_7	3
l_8	6	w_8	1

4.Results

A smaller VSWR value enables better antenna matching to the transmission line and greater power provided to the load. Scattering parameter (S11) contributes to determining the mismatch from the termination in terms of energy returned back to the radiating source. Gain of antenna is the amount of power transferred in the peak radiation direction as compared to an isotropic antenna. *Figure 2* depicts the quintuple band antenna's predicted return loss S11

at 21 GHz, 24 GHz, 28 GHz, 31 GHz, and 34 GHz. The planned antenna radiated optimally at 21 GHz, 24 GHz, 28 GHz, 31 GHz, and 34 GHz. S11 was -13.39 dB at 21 GHz, -14.73 dB at 24 GHz, -13.82 dB at 28 GHz, -10 dB at 31 GHz, and -17.94 dB at 34 GHz in vicinity of these best-performing frequencies. According to *Figure 2*, the reflection coefficient ranges from -10 dB to -17 dB at the resonant frequencies.

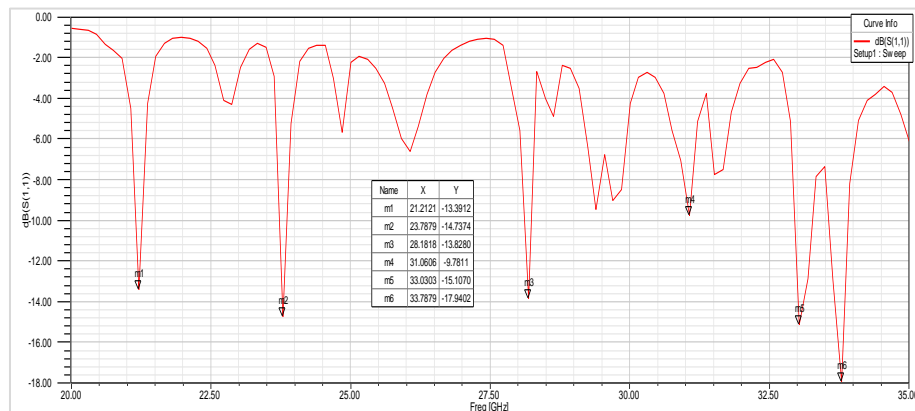


Figure 2 Reflection coefficient S11 for the quintuple resonant frequency stands at -13.39 dB at 21 GHz, -14.73 dB at 24 GHz, -13.82 dB at 28 GHz, -10 dB at 31 GHz and -17.94 dB at 34 GHz

Over whole frequency range, the port isolation was superior to 13 dB. The simulation result reported 6 dBi gain. A portion of energy is returned back towards the radiator in actual systems due to mismatched impedances. *Figure 3* depicts the plot of VSWR against the operational frequency. From the simulation graph, at frequencies 21GHz, 24 GHz, 28 GHz, 31 GHz and 33 GHz, the VSWR value of 1.54, 1.44, 1.44, 1.9 and 1.42 respectively was obtained, all as per the ideal requirement. The frequency range across which an antenna matches a certain parameter

specification is known as its bandwidth. The recommended antenna showed impedance bandwidth of roughly 0.5 GHz. *Figures 4* and *Figure 5*, respectively, exhibit the E-plane and three-dimensional radiation patterns. An antenna's electric field and magnetic field plane patterns are frequently characterised in terms of the plane of polarisation of an electromagnetic wave. In some cases, the H-plane pattern can be interpreted as an azimuth pattern, whereas the E-plane pattern might be seen as an elevation pattern.

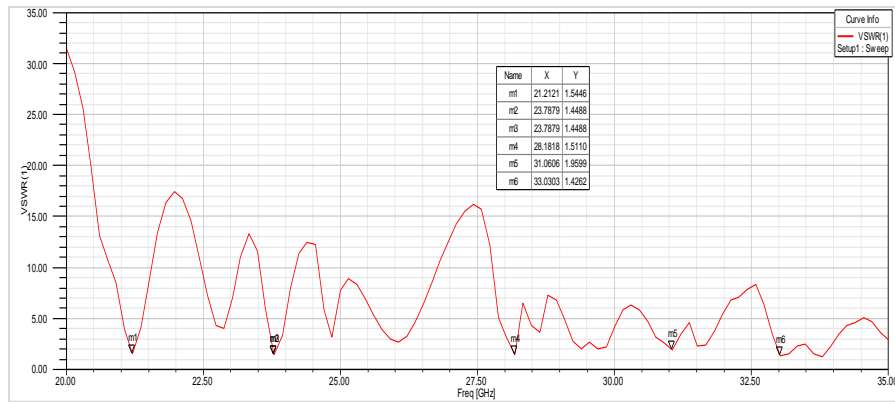
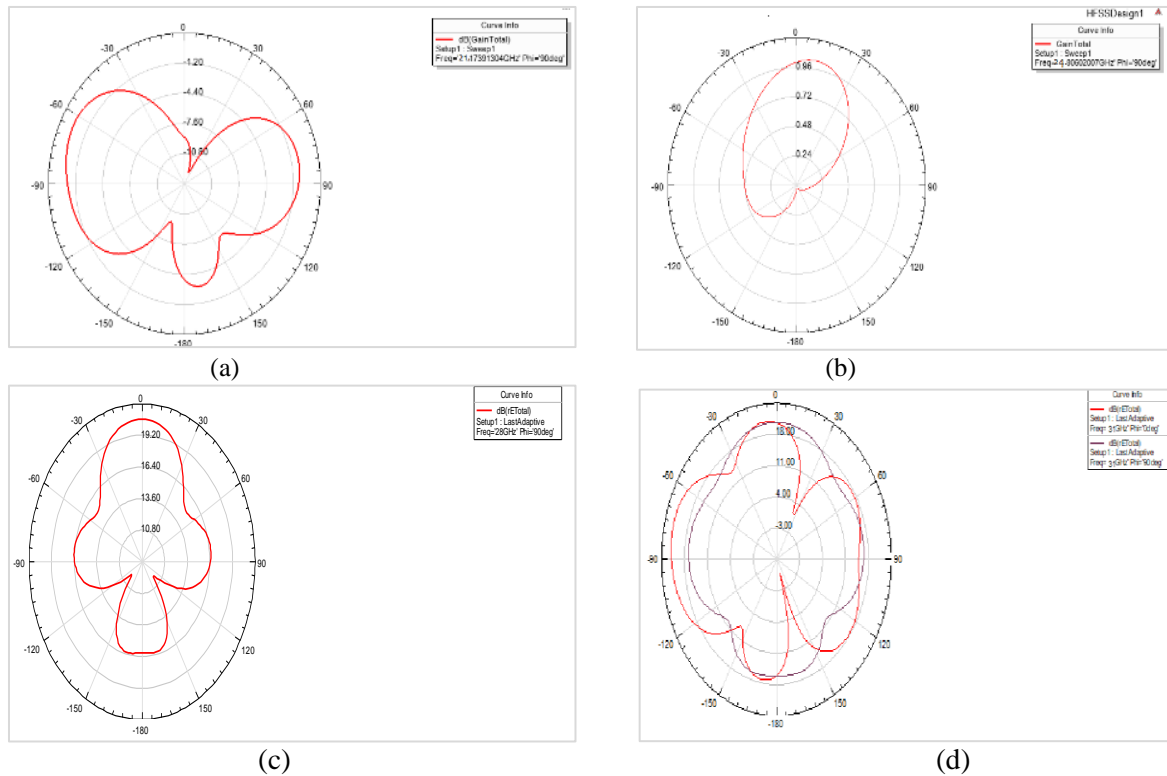
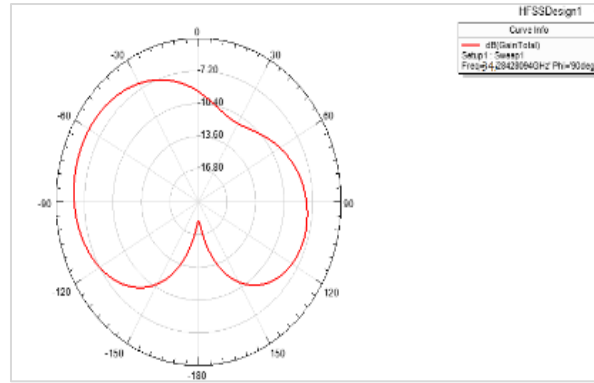


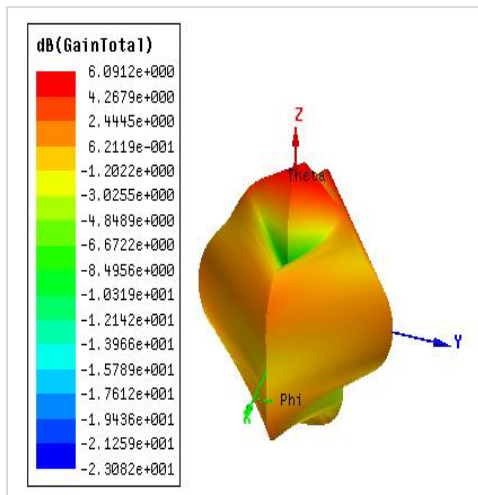
Figure 3 VSWR values obtained at quintuple resonant frequencies 21 GHz, 24 GHz, 28 GHz, 31 GHz and 33 GHz are 1.54, 1.44, 1.44, 1.9 and 1.42 respectively



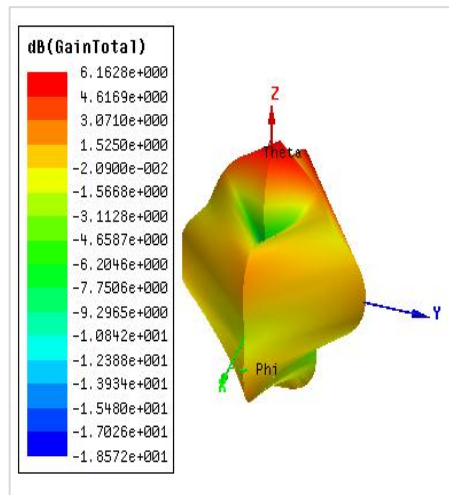


(e)

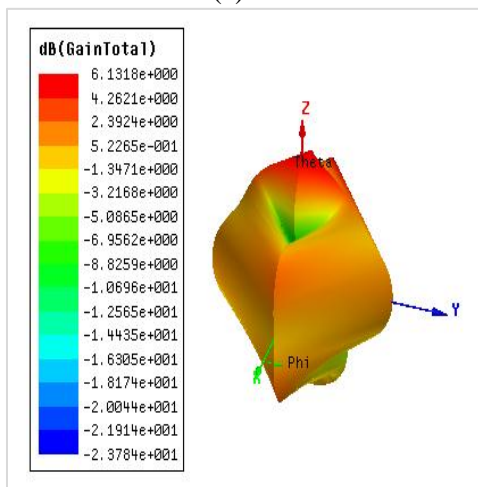
Figure 4 2D radiation pattern: (a) resonant frequency 21 GHz, $\varphi = 90^\circ$, (b) resonant frequency 24 GHz, $\varphi = 90^\circ$, (c) resonant frequency 28 GHz, $\varphi = 90^\circ$, (d) resonant frequency 31 GHz, $\varphi = 90^\circ$ and (e) resonant frequency 34 GHz, $\varphi = 90^\circ$



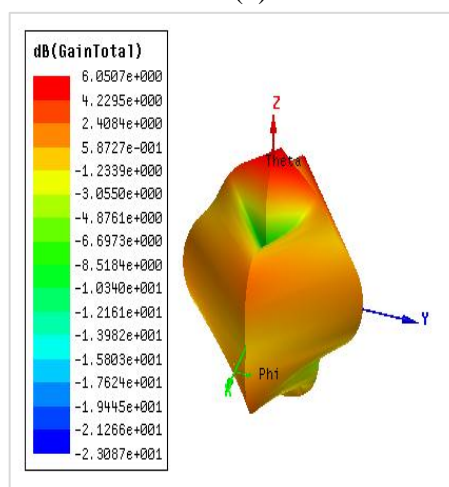
(a)



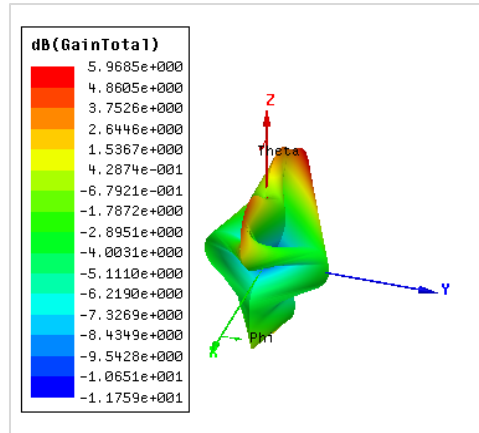
(b)



(c)



(d)



(e)

Figure 5 Antenna gain at frequency (a) 21 GHz, (b) 24 GHz, (c) 28 GHz, (d) 31 GHz, and (e) 34 GHz

Antenna gain, $10 \times \log(P_o/P_i)$, measured in dB, refers to an antenna's capacity of directional emission compared to ideal antenna. High directional emission antennas provide increased range in a certain direction but require precision aiming. Low gain antennas are designed to receive electromagnetic signals from all available directions, but their range is

restricted. Admittance is an imaginary quantity. *Figure 6* and *Figure 7* display real and imaginary Y parameter against operational frequency. The real Y vs frequency plot produced two good conductance values, 0.5385 and 0.8729. The antenna may be effectively used at frequencies about 28 GHz with an obtained susceptance of -0.0318.

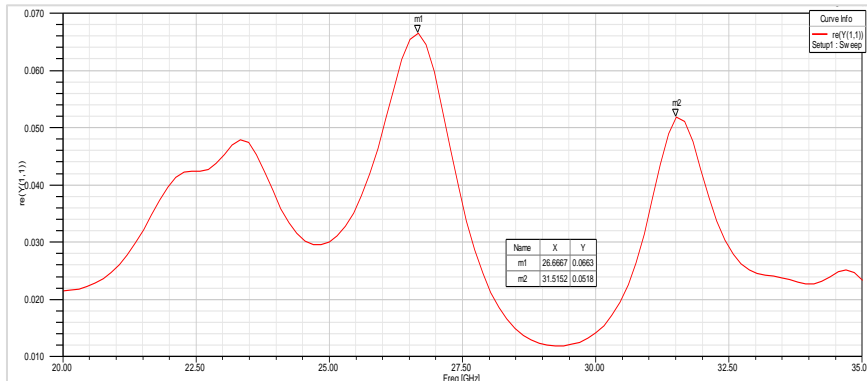


Figure 6 Y-parameter (Re)

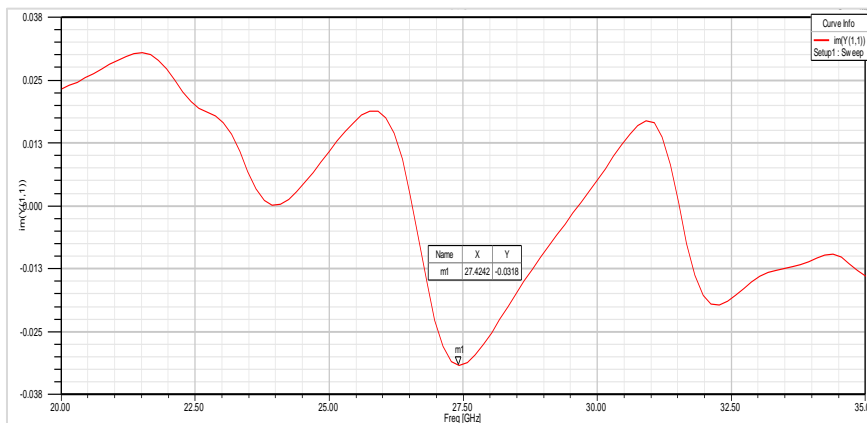


Figure 7 Y-parameter (Im)

An antenna with a directivity of 1 (0 dB) would be omni-directional and radiate equally well in all directions. The more focused an antenna's beam is, the higher its directivity. *Figure 8* displays the results

of directivity of antenna due to simulation. Better directivity was realized at the multiple resonant frequency enabling antenna to radiate equally well in all directions.

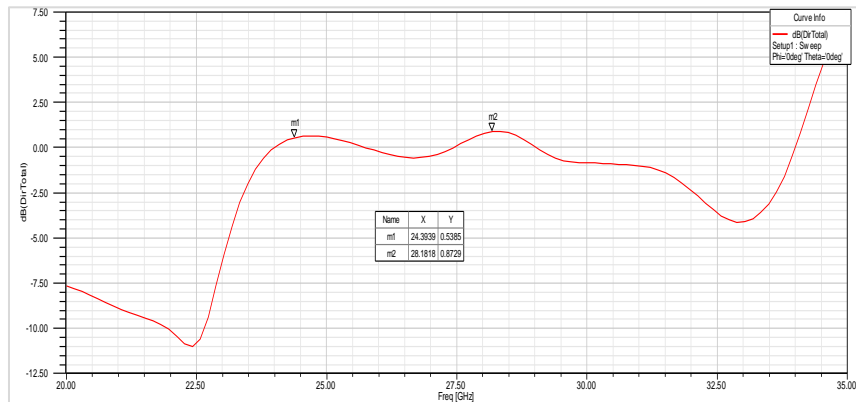


Figure 8 Directivity

Figure 9 depicts the photograph of the antenna prototype. Both frontal and rear view are shown which are identical with the simulation design on HFSS. Prototype was fabricated and tested to validate the obtained results. Laboratory measurement of antenna prototype was done with VNA. System-in-

packages (SiPs) can be used to integrate antennas with wireless communications equipment. SiPs have the intrinsic benefit of avoiding antenna detuning issues, which are frequently linked with tiny AI, IoT devices, and other 5G/6G mobile communication systems.

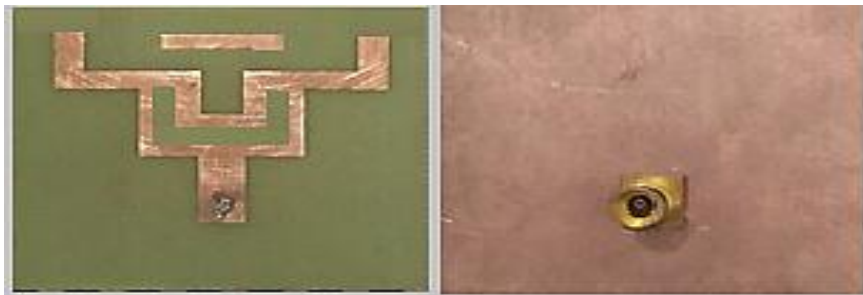


Figure 9 Antenna prototype

Measurement results were obtained by termination of antenna with a 50-ohm load on a transmission-line model with co-axial feeding of signals. The simulated and fabricated results were compared. *Table 2* lists the results value due to simulation and laboratory measurement. Simulated reflection coefficient at quintuple frequencies 21 GHz, 24 GHz, 28 GHz, 31 GHz and 34 GHz were -13.39 dB, -14.73 dB, -13.83 dB, -10.00 dB and -17.94 dB whereas the compared measured values were found to be -14.00 dB, -16.00 dB, -15.00 dB, -11.00 dB and -15.00 dB. VSWR from the simulations were 1.54, 1.44, 1.44, 1.90 and 1.42 whereas those from the measurement turned out to be 1.70, 1.50, 1.30, 1.40 and 1.70. Gain obtained from simulation for the resonant frequencies were

6.09 dB, 6.16 dB, 6.13 dB, 6.05 dB and 5.21 dB and that obtained from the measurement were respectively 5.80 dB, 6.30 dB, 5.70 dB, 6.20 dB and 5.98 dB, which almost compared. Plots of reflection coefficient S11, VSWR and gain are shown in *Figures 10, 11* and *12* respectively, based on the measured values of the prototype. The observed results for VSWR and S11 closely matched the simulated values. The minor deviation between the simulation and laboratory measurement results could still be assigned to prototype development tolerance, integration of the coaxial feed with the antenna, measurement conditions, and sensitivity to ambient temperature or physical stress that may have occurred during the physical moulding of the antenna.

Table 2 Parameter analysis

S. No.	Parameter	Result	21 GHz	24 GHz	28 GHz	31 GHz	34 GHz
1.	S11(dB)	Simulated	-13.39	-14.73	-13.83	-10.00	-17.94
		Measured	-14.00	-16.00	-15.00	-11.00	-15.00
2.	VSWR	Simulated	1.54	1.44	1.44	1.90	1.42
		Measured	1.70	1.50	1.30	1.40	1.70
3.	Gain (dB)	Simulated	6.09	6.16	6.13	6.05	5.21
		Measured	5.8	6.3	5.7	6.2	5.98

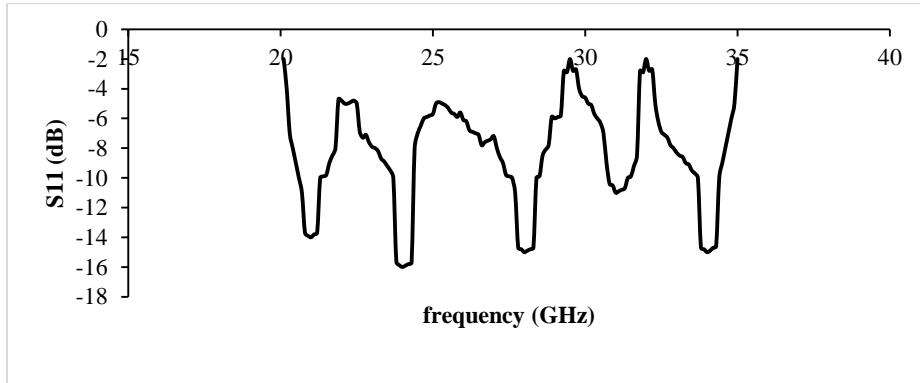


Figure 10 Return loss of the prototype

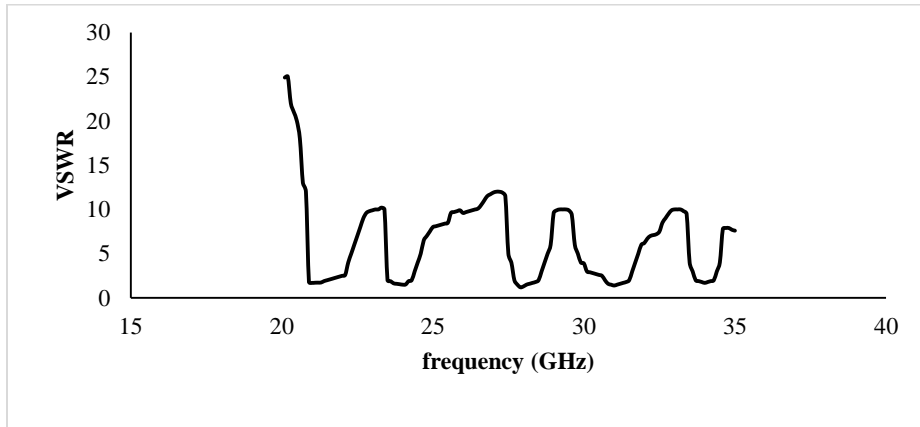


Figure 11 VSWR of the prototype

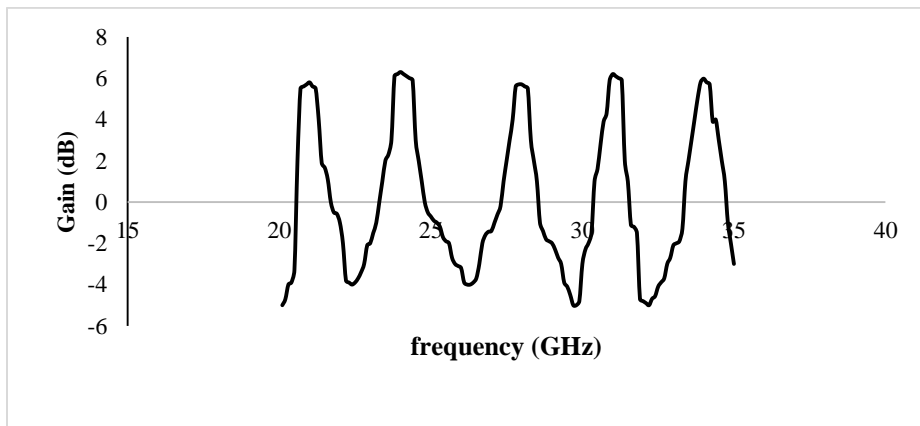


Figure 12 Measured values of Gain of the prototype

5. Discussion

This study sought to help achieve multiple band operating characteristics in a planar millimetre wave antenna using HFSS design, modelling, and prototype construction of the proposed antenna. Quintuple (five) bands of operation have been achieved with acceptable parametric values and a steady radiation pattern for the device working in the K-band frequency ranges of millimeter wave communication. As a result, the current research is significant in developing improved solutions for the demands of multifrequency operation, namely five bands, of antennas for millimetre wave communication.

The resultant parameters of the proposed antenna showed that the antenna resonates at the designing frequencies 21 GHz, 24 GHz, 28 GHz, 31 GHz, and 34 GHz. *Table 3* compares the current work data to previously published works. Findings of the study were compared with the previous significant research on quintuple bands, most of which used an FR4 substrate. One four-band and one three-band result were also included for uniformity. The comparison was based on antenna size, operating frequencies, dielectric material, and antenna gain. It is clear that the suggested antenna provides a number of advantages, including multiband function, multi-polarization capabilities, a relatively small size, easy and simple construction and a reasonably good gain across the pentaband.

Table 3 Comparison of the suggested antenna with other published multiband antennas

Papers	Frequency band	Size of Antenna (mm)	Operating frequency (GHz)	Material used	Gain(dBi)
[48]	Four band	30×40	2.5, 4.5, 5.7, 7.7	RT/Duroid 5880	2.13, 2.27, 2.56, 5.33
[49]	Five band	27.4×24	2.5, 3.5, 4.6, 6.1, 7.5	FR4 substrate	1.41, 2.1, 2.3, 1.82, 2.92
[50]	Five band	14.6×10.8	27.8, 30.3, 40.1, 47.2, 56.7	Polytetrafluoroethylene (PTFE)	10.2, 8.4, 7.7, 9.5, 8.4
[51]	Three band	4.4×6.6	28, 40, 47	FR4 epoxy	5.64, 8.7, 6.17
This work	Five band	28×25	21, 24, 28, 31, 34	FR4 substrate	5.8, 6.3, 5.7, 6.2, 5.98

5.1 Overall analysis and impact of the results

The antenna has two U-shaped and L-shaped slots, as well as a parasitic slot. The Ansoft HFSS electromagnetic simulator was used to perform simulation, followed by laboratory measurements using the built prototype. The results of the antenna parameters obtained through simulation steps have striking resemblance with those realised by the actual laboratory measurements on the developed prototype of the designed antenna. Good return loss has been attained, implying that the reflected signals will have no effect on the supplied signal. The patch delivers maximum power. Sufficient impedance matching was obtained. A bandwidth of 0.5 GHz and a VSWR value less than 1.6 are suitable for commercial integration of the device. A gain of 6.13 dB may give a good combination of range and ability of connection with adjacent radiators. Gain has a strong match between measured and simulated findings, notably at 21 GHz, with a decent agreement for the other four frequencies. The modelling and observed findings matched nearly perfectly, with values similar to those required for mm wave wireless communication. This certifies planned antenna useful for multiband operation and applications.

5.2 Limitations

The proposed antenna operates at five new frequencies in K band. Higher multiband frequency operation could not be investigated with the specified antenna dimensions because high frequency antenna dimensions are further lowered to nanoscale, to which the authors have no technological access. The performance of antennas in various environmental circumstances such as temperature changes, humidity, and physical stress is outside the scope of this work and will be studied further in the future.

A complete list of abbreviations is listed in *Appendix I*.

6. Conclusion and future work

A five-band MPA with parasitic element built on the HFSS platform was investigated. The simulation findings in terms of S11, VSWR, and gain were consistent with the observed data obtained from the prototype built. The suggested antenna was printed on FR4 and is competitively priced. Quintuple bands (five bands) of frequency operation were achieved at 21 GHz, 24 GHz, 28 GHz, 31 GHz, and 34 GHz for

5G and beyond millimetre wireless communication equipment. For all five frequency bands, the simulated and measured VSWR and S11 findings agreed perfectly. The antenna gain is reasonably matched. The antenna's performance meets the criteria of 5G/6G mobile communication in the K band (18 GHz to 27 GHz) and, to some extent, the Ka band (27 GHz to 40 GHz). Following the results, it is discovered that FR4 material is appropriate as a substrate for realising quintuple band antenna functioning. It has also been noted that the slots as parasitic elements enhance antenna characteristics. The suggested antenna is appropriate for satellite communication, including military and defence applications. Future research might look at how antennas work under various environmental circumstances, including as temperature changes, humidity, and physical stress.

Acknowledgment

Authors extend heartfelt gratitude to Prof. Mona Priya, Department of EEE, Nalanda College of Engineering, Nalanda, Bihar, India for her unwavering support and cooperation during the work.

Conflicts of interest

The authors have no conflicts of interest to declare.

Data availability

None

Author's contribution statement

Kumari Mamta: Conceptualization, design, investigation and correspondence. **Raj Kumar Singh:** Review, measurements, analysis, manuscript preparation and editing.

References

- [1] Saxena S, Kanaujia BK, Dwari S, Kumar S, Tiwari R. A compact microstrip fed dual polarised multiband antenna for IEEE 802.11 a/b/g/n/ac/ax applications. *AEU-International Journal of Electronics and Communications*. 2017; 72:95-103.
- [2] Singh DK, Kanaujia B, Dwari S, Pandey GP, Kumar S. Multiband circularly polarized stacked microstrip antenna. *Progress in Electromagnetics Research C*. 2015; 56:55-64.
- [3] Giri KK, Singh RK, Mamta K. Multiband antenna design for modern wireless communication system. In 4th international conference on recent trends in computer science and technology 2022 (pp. 364-8). IEEE.
- [4] Chen ZN, Qing X. Dual-band circularly polarized S-shaped slotted patch antenna with a small frequency-ratio. *IEEE Transactions on Antennas and Propagation*. 2010; 58(6):2112-5.
- [5] Mamta K, Singh RK. Analysis of reconfigurable polarisation antenna as an EMI sensor. *British Journal of Applied Science & Technology*. 2017; 19(5):1-8.
- [6] Lee KF, Tong KF. Microstrip patch antennas—basic characteristics and some recent advances. *Proceedings of the IEEE*. 2012; 100(7):2169-80.
- [7] Cui Y, Wang X, Shen G, Li R. A triband SIW cavity-backed differentially fed dual-polarized slot antenna for WiFi/5G applications. *IEEE Transactions on Antennas and Propagation*. 2020; 68(12):8209-14.
- [8] Waterhouse R. Microstrip patch antennas. In *handbook of antennas in wireless communications*. CRC Press; 2018.
- [9] Malik PK, Padmanaban S, Holm-nielsen JB. Microstrip antenna design for wireless applications. CRC Press; 2021.
- [10] Soni D, Yadav D, Tiwari M. Wideband, sand-timer-shaped antenna for 5G mm wave and 28 GHz applications. *International Journal of Intelligent Systems and Applications in Engineering*. 2024; 12(4s):685-90.
- [11] Davoudabadifarhahi H, Ghalamkari B. High efficiency miniaturized microstrip patch antenna for wideband terahertz communications applications. *Optik*. 2019; 194:163118.
- [12] Gatram M, Karumuri R. Design of DNG metamaterial loaded single fed wideband microstrip patch antenna at 28 GHz for millimeter wave applications. *Tuijin Jishu/Journal of Propulsion Technology*. 2024; 45(1):1-8.
- [13] Belen MA. Performance enhancement of a microstrip patch antenna using dual-layer frequency-selective surface for ISM band applications. *Microwave and Optical Technology Letters*. 2018; 60(11):2730-4.
- [14] Dhakad SK, Prasad A, Dwivedi U. Design of a miniaturized microstrip patch antenna for triple-band operation in X, Ku and K band with band-notch characteristics. In international conference on power, control, signals and instrumentation engineering 2017 (pp. 2235-40). IEEE.
- [15] Chao Z, Zitong Z, Pei X, Jie Y, Zhu L, Gaosheng L. A miniaturized microstrip antenna with tunable double band-notched characteristics for UWB applications. *Scientific Reports*. 2022; 12(1):1-13.
- [16] Singh D, Choudhary SD, Mohapatra B. Design of microstrip patch antenna for Ka-band (26.5-40 GHz) applications. *Materials Today: Proceedings*. 2021; 45:2828-32.
- [17] Lee KF, Luk KM, Lai HW. *Microstrip patch antennas*. World Scientific; 2017.
- [18] Uwaechia AN, Mahyuddin NM. A comprehensive survey on millimeter wave communications for fifth-generation wireless networks: feasibility and challenges. *IEEE Access*. 2020; 8:62367-414.
- [19] Kandwal A. Compact dual band antenna design for Ku/Ka band applications. *Advanced Electromagnetics*. 2017; 6(4):1-5.
- [20] Darimireddy NK, Reddy RR, Prasad AM. Design of triple-layer double U-slot patch antenna for wireless

- applications. *Journal of Applied Research and Technology*. 2015; 13(5):526-34.
- [21] Alibakhshi-kenari M, Naser-moghadasi M, Sadeghzadeh RA, Virdee BS, Limiti E. New CRLH-based planar slotted antennas with helical inductors for wireless communication systems, RF-circuits and microwave devices at UHF–SHF bands. *Wireless Personal Communications*. 2017; 92:1029-38.
- [22] Tan Q, Chen FC. Triband circularly polarized antenna using a single patch. *IEEE Antennas and Wireless Propagation Letters*. 2020; 19(12):2013-7.
- [23] Alibakhshikenari M, Limiti E, Naser-moghadasi M, Virdee BS, Sadeghzadeh RA. A new wideband planar antenna with band-notch functionality at GPS, bluetooth and WiFi bands for integration in portable wireless systems. *AEU-International Journal of Electronics and Communications*. 2017; 72:79-85.
- [24] Alibakhshi-kenari M, Naser-moghadasi M, Sadeghzadeh R. The resonating MTM-based miniaturized antennas for wide-band RF-microwave systems. *Microwave and Optical Technology Letters*. 2015; 57(10):2339-44.
- [25] Li E, Li XJ, Zhao Q. A design of ink-printable triband slot microstrip patch antenna for 5G applications. In 4th Australian microwave symposium 2020 (pp. 1-12). IEEE.
- [26] Asif S, Iftikhar A, Rafiq MN, Braaten BD, Khan MS, Anagnostou DE, et al. A compact multiband microstrip patch antenna with U-shaped parasitic elements. In *IEEE international symposium on antennas and propagation & USNC/URSI national radio science meeting 2015* (pp. 617-8). IEEE.
- [27] Ata OW, Salamin M, Abusabha K. Double U-slot rectangular patch antenna for multiband applications. *Computers & Electrical Engineering*. 2020; 84:106608.
- [28] Khunead G, Nakasuwan J, Songthanapitak N, Anantrasirichai N. Investigate rectangular slot antenna with L-shape strip. *Piers online*. 2007; 3(7):1076-9.
- [29] Wang D, Wong H, Ng KB, Chan CH. Wideband shorted higher-order mode millimeter-wave patch antenna. In *proceedings of the international symposium on antennas and propagation 2012* (pp. 1-2). IEEE.
- [30] Gaid AS, Ali MA, Saif A, Mohammed WA. Design and analysis of a low profile, high gain rectangular microstrip patch antenna for 28 GHz applications. *Cogent Engineering*. 2024; 11(1):2322827.
- [31] Anooz RSA, Ammar BK. A modified ground for bandwidth enhancement of the microstrip patch antenna for 5G wireless communications. *SSRG International Journal of Electrical and Electronics Engineering*. 2024; 11(2):19-23.
- [32] Balanis CA. *Antenna theory: analysis and design*. John Wiley & sons; 2016.
- [33] Senthilkumar S, Udhayanila K, Mohan V, Senthil KT, Devarajan D, Chitrakala G. Design of microstrip antenna using high frequency structure simulator for 5G applications at 29 GHz resonant frequency. *International Journal of Advanced Technology and Engineering Exploration*. 2022; 9(92):996-1008.
- [34] Zhu S, Liu H, Chen Z, Wen P. A compact gain-enhanced vivaldi antenna array with suppressed mutual coupling for 5G mmwave application. *IEEE Antennas and Wireless Propagation Letters*. 2018; 17(5):776-9.
- [35] Khalily M, Tafazolli R, Xiao P, Kishk AA. Broadband mm-wave microstrip array antenna with improved radiation characteristics for different 5G applications. *IEEE Transactions on Antennas and Propagation*. 2018; 66(9):4641-7.
- [36] Dzagbletey PA, Jung YB. Stacked microstrip linear array for millimeter-wave 5G baseband communication. *IEEE Antennas and Wireless Propagation Letters*. 2018; 17(5):780-3.
- [37] Yoon N, Seo CA. A 28-GHz Wideband 2×2 U-slot patch array antenna. *Journal of Electromagnetic Engineering and Science*. 2017; 17(3):133-7.
- [38] Tang MC, Shi T, Ziolkowski RW. A study of 28 GHz, planar, multilayered, electrically small, broadside radiating, Huygens source antennas. *IEEE Transactions on Antennas and Propagation*. 2017; 65(12):6345-54.
- [39] Diawuo HA, Jung YB. Broadband proximity-coupled microstrip planar antenna array for 5G cellular applications. *IEEE Antennas and Wireless Propagation Letters*. 2018; 17(7):1286-90.
- [40] Sehrai DA, Khan J, Abdullah M, Asif M, Alibakhshikenari M, Virdee B, et al. Design of high gain base station antenna array for mm-wave cellular communication systems. *Scientific Reports*. 2023; 13(1):1-8.
- [41] Sehrai DA, Asif M, Shoaib N, Ibrar M, Jan S, Alibakhshikenari M, et al. Compact quad-element high-isolation wideband MIMO antenna for mm-wave applications. *Electronics*. 2021; 10(11):1-10.
- [42] Mohammed AS, Kamal S, Ain MF, Hussin R, Najmi F, Sundi SA, et al. Mathematical model on the effects of conductor thickness on the centre frequency at 28 GHz for the performance of microstrip patch antenna using air substrate for 5G application. *Alexandria Engineering Journal*. 2021; 60(6):5265-73.
- [43] Devana VK, Beno A, Alzaidi MS, Krishna PB, Divyamrutha G, Awan WA, et al. A high bandwidth dimension ratio compact super wide band-flower slotted microstrip patch antenna for millimeter wireless applications. *Heliyon*. 2024; 10(1):1-9.
- [44] Sharaf MH, Zaki AI, Hamad RK, Omar MM. A novel dual-band (38/60 GHz) patch antenna for 5G mobile handsets. *Sensors*. 2020; 20(9):1-19.
- [45] Pimienta-del-valle D, Mendo L, Riera JM, Garcia-del-pino P. Indoor LOS propagation measurements and modeling at 26, 32, and 39 GHz millimeter-wave frequency bands. *Electronics*. 2020; 9(11):1-16.
- [46] Bangash K, Ali MM, Maab H, Ahmed H. Design of a millimeter wave microstrip patch antenna and its array for 5g applications. In *international conference on electrical, communication, and computer engineering 2019* (pp. 1-6). IEEE.

- [47] Mane PR, Kumar P, Ali T, Alsath MG. Planar MIMO antenna for mmwave applications: evolution, present status & future scope. *Heliyon*. 2023; 9(2):1-32.
- [48] Kumar A, Deegwal JK, Sharma MM. Design of multi-polarised quad-band planar antenna with parasitic multistubs for multiband wireless communication. *IET Microwaves, Antennas & Propagation*. 2018; 12(5):718-26.
- [49] Fertas F, Challal M, Fertas K. Miniaturized quintuple band antenna for multiband applications. *Progress in Electromagnetics Research M*. 2020; 89:83-92.
- [50] Dejen A, Ridwan M, Jayasinghe J, Anguera J. Multi-band mm-wave wearable antenna synthesized with a genetic algorithm. *International Journal of Antennas and Propagation*. 2022; 2022:1-17.
- [51] Dejen A, Jayasinghe J, Ridwan M, Anguera J. Genetically engineered tri-band microstrip antenna with improved directivity for mm-wave wireless application. *AIMS Electronics and Electrical Engineering*. 2022; 6(1):1-15.



Kumari Mamta has obtained her Ph.D. degree from Ranchi University, in the year 2011. Currently she is in the Department of Applied Science and Humanities, Nalanda College of Engineering, Nalanda, India as Associate Professor of Physics. Her chief research interest lies in the field of Radiating Structures using Numerical Methods, Computations and Virtual Simulations. Dr. Mamta has been Erasmus Mundus India4EUII Post-Doctoral fellow with Department of Electromagnetic Engineering at Politecnico di Torino, Italy, funded by the European Commission.

Email: mamta.singh548@gmail.com



Raj Kumar Singh obtained Ph.D. degrees in Physics from Ranchi University, Ranchi, in the year 2013. Since 2008, he has been an Assistant Professor with the Physics Department, RU, Ranchi. His research interests are in the field of Spin Polarization, Spin Memory And Devices, Electromagnetic Radiating Structures using Numerical Methods, Computations And Simulations. Dr. Singh has been Erasmus Mundus Post-Doctoral fellow at Politecnico di Torino, Italy, funded by the European Commission.

Email: rajkrsingh08@gmail.com

Appendix I

S. No.	Abbreviation	Description
1	5G	Fifth Generation
2	6G	Sixth Generation
3	AI	Artificial Intelligence
4	CNC	Computerized Numerical Control
5	CP	Circularly Polarized
6	CPW	Coplanar Waveguide
7	CST	Computer Simulation Technology
8	dB	Decibel
9	dBi	decibel relative to isotropic
10	FTBR	Front-to-Back Ratio
11	FR4	Fire Retardant 4
12	GPS	Global Positioning System
13	HP	Hewlett-Packard
14	HTS	High Throughput Satellite
15	HFSS	High Frequency Structure Simulator
16	IoT	Internet of Things
17	ITS	Intelligent Transportation Systems
18	LP	Linearly Polarised
19	MIMO	Multiple-input-multiple-output
20	MPA	Microstrip Patch Antenna
21	PCB	Printed Circuit Board
22	PTFE	Polytetrafluoroethylene
23	RF	Radio Frequency
24	S11	Scattering Parameter 11/Return Loss/Reflection Coefficient
25	SiPs	System in Packages
26	TLC	Taconic Thin Layer Chromatography
27	VNA	Vector Network Analyzer
28	VSAT	Very Small Aperture Terminal
29	VSWR	Voltage Standing Wave Ratio
30	WiFi	Wireless Fidelity
31	WiMAX	Worldwide Interoperability for Microwave Access
32	WLAN	Wireless Local Area Network